Characterization of ^{68}Ga-DOTA-D-Phe^1-Tyr^3-Octreotide Kinetics in Patients with Meningiomas

Marcus Henze, MD[1]; Antonia Dimitrakopoulou-Strauss, MD[2]; Stefanie Milker-Zabel, MD[3]; Jochen Schuhmacher, PhD[4]; Ludwig G. Strauss, MD[2]; Josef Doll, PhD[5]; Helmut R. Mäcke, PhD[6]; Michael Eisenhut, PhD[4]; Jürgen Debus, MD[3]; and Uwe Haberkorn, MD[1,2]

[1]Department of Nuclear Medicine, University of Heidelberg, Heidelberg, Germany; [2]Clinical Cooperation Unit Nuclear Medicine, German Cancer Research Center, Heidelberg, Germany; [3]Department of Radiation Oncology, University of Heidelberg, Heidelberg, Germany; [4]Division of Radiochemistry and Radiopharmacology, German Cancer Research Center, Heidelberg, Germany; [5]Department of Innovative Cancer Diagnostics and Therapy, German Cancer Research Center, Heidelberg, Germany; and [6]University Hospital Basel, Basel, Switzerland

Because biopsy has a high risk of hemorrhage and the findings of CT and MRI are often ambiguous, especially at the base of the skull, additional methods for the characterization of intracranial tumors are needed. Meningiomas show high expression of the somatostatin receptor subtype 2 and thus offer the possibility of receptor-targeted imaging. We used the somatostatin analog ^{68}Ga-DOTA-D-Phe^1-Tyr^3-octreotide (DOTA-TOC) labeled with the positron emitter ^{68}Ga (half-life, 68 min), obtained from a ^{68}Ge/^{68}Ga generator, for PET of these tumors. In contrast to ^{18}F-FDG, this ligand shows high meningioma-to-background ratios. The aim was to evaluate kinetic parameters in meningiomas before radiotherapy. **Methods:** Dynamic PET scans (3-dimensional mode; 28 frames; ordered-subsets expectation maximization reconstruction) were acquired for 21 patients (mean age ± SD, 51 ± 13 y) before radiotherapy during the 60 min after intravenous injection of 156 ± 29 MBq of ^{68}Ga-DOTA-TOC. We analyzed 28 meningiomas (median grade [I] according to the system of the World Health Organization) with volumes of at least 0.5 mL (mean volume, 13.1 mL) and nasal mucosa as reference tissue, showing a slight to moderate physiologic uptake. For evaluation of the ^{68}Ga-DOTA-TOC kinetics, the vascular fraction (vB) and the rate constants (k1, k2, k3, and k4 [1/min]) were computed using a 2-tissue-compartment model. Furthermore, receptor binding (RB) (k1 − k1 × k2) and the ratios k1/k2 and k3/k4 were calculated. **Results:** Significant differences ($P < 0.05$; t test) between meningiomas and the reference tissue were found for the mean standardized uptake value (10.5 vs.1.3), vB (0.42 vs. 0.11), k2 (0.12 vs. 0.56), k3 (0.024 vs. 0.060), k4 (0.004 vs. 0.080), and RB (0.49 vs. 0.13). Although there was no significant difference for k1 (0.54 vs. 0.40), the ratios k1/k2 (4.50 vs. 0.71) and k3/k4 (6.00 vs. 0.75) were markedly greater in meningiomas than in reference tissue. **Conclusion:** The high uptake of ^{68}Ga-DOTA-TOC in meningiomas can be explained by the high values for vB and by the remarkably low values for k2 and k4, leading to significantly greater k1/k2 and k3/k4 ratios and RB in meningiomas than in reference tissue. Thus, pharmacokinetic modeling offers a more detailed analysis of biologic properties of meningiomas. In further studies, these data might serve as a basis for monitoring the somatostatin receptors of meningiomas after radiotherapy.

Key Words: somatostatin receptors; ^{68}Ga-DOTA-TOC; PET; kinetic modeling; meningioma

Meningiomas are mesodermal tumors originating in the arachnoid membrane. The incidence is approximately 2.5 per 100,000 people and increases with age. Meningiomas represent 15%–20% of intracranial neoplasms in adults, with a clear predomination in women (1). More than 90% of intracranial meningiomas are slow growing and histopathologically benign. Surgical resection is the preferred treatment whenever total removal can be accomplished with acceptable morbidity rates. Because complete resection is often impossible at the base of the skull, the role of radiosurgery increases as primary or adjuvant treatment. When morphologic imaging methods such as CT or MRI are used for skull-base tumors, differentiation between meningioma, neurinoma/neurofibromas, and metastases is often difficult, and biopsy has a high risk of hemorrhage. Alternative methods for the characterization of these tumors are needed.

Meningiomas show expression of a variety of receptors, including progesterone, androgen, platelet-derived growth factor, epidermal growth factor, prolactin, dopamine, and somatostatin receptor (SSTR) subtype 2 (SSTR2) (1,2). Somatostatin is ubiquitously distributed in the body, inhibiting various hormonal systems and physiologic functions. Five receptor subtypes (SSTR1–5), acting through transmembrane domain G proteins, have been identified. SSTRs are overexpressed in many tumors (e.g., in neuroendocrine, lung, and breast tumors and in lymphomas), with subtype specificity for each histology. ^{111}In-Diethylenetriaminepentaacetic acid (DTPA)-octreotide SPECT is a valuable technique for

differentiating between meningiomas, neurinomas, and neurofibromas and for the postsurgical follow-up of meningioma patients (*3*). Furthermore, SSTR imaging was helpful for distinguishing between meningiomas and pituitary adenomas on the basis of qualitative tracer uptake (*3*). A major drawback of ^{111}In-DTPA-octreotide SPECT is the difficulty of detecting meningiomas with a diameter of less than 2.7 cm or a volume of less than 10 mL (*4*).

Recently, the somatostatin analog DOTA-D-Phe[1]-Tyr[3]-octreotide (DOTA-TOC) has been developed (*5*). 1,4,7,10-Tetraazacyclododecane-*N,N′,N″,N‴*-tetraacetic acid (DOTA) is a macrocyclic chelator that ensures high in vivo stability for the corresponding radiometal chelates. Replacing Phe[3] by Tyr in the octapeptide increases its hydrophilicity and thus the efficiency of its clearance by the kidney and leads to an enhanced affinity for the human SSTR2 (*5,6*).

Because of the increased spatial resolution and the ability to quantify biodistribution, PET is desirable for SSTR imaging. For that reason, DOTA-TOC has been labeled with the positron emitter [68]Ga. ^{68}Ga-DOTA-TOC is of value for scintigraphic evaluation of patients with SSTR-positive lesions such as neuroendocrine tumors, especially carcinoids (*7–9*). In contrast to, for example, ^{18}F-FDG, ^{68}Ga-DOTA-TOC showed high meningioma-to-background ratios. It provided valuable additional information on the extent of meningiomas beneath osseous structures, especially at the skull base (*10*).

The purpose of this study was to gather basic information about the kinetic behavior of the novel compound ^{68}Ga-DOTA-TOC in previously nonirradiated low-grade meningiomas. The kinetic parameters of ^{68}Ga-DOTA-TOC in meningioma patients were determined by pharmacokinetic modeling of dynamic PET scans.

MATERIALS AND METHODS

^{68}Ga-DOTA-TOC

DOTA-TOC was synthesized as described in the literature (*5*). The labeling procedure is easy, takes less than 1 h, and results in radiochemical yields greater than 96%. [68]Ga (half-life [$t_{1/2}$], 68 min) for peptide labeling was obtained from a [68]Ge/^{68}Ga generator that consists of a column containing a self-made pyrogallol-formaldehyde copolymer loaded with [68]Ge and coupled with a small anion exchanger column (AG 1 × 8; BioRad) to concentrate ^{68}Ga during elution (*11*). The eluate, containing ^{68}Ga in 0.2 mL of HCl (0.5 mol/L), was evaporated to dryness and redissolved in 200 μL of acetate buffer (0.1 mol/L; pH 4.8). ^{68}Ga-DOTA-TOC was prepared by adding 14 μL of aqueous DOTA-TOC solution (1 mmol/L) and heating the mixture for 15 min at 95°C. Uncomplexed ^{68}Ga was separated by adsorption on a reversed-phase cartridge (Sep-Pak; Waters Corp.), which was equilibrated with acetate buffer (0.1 mol/L; pH 6.2), whereas ^{68}Ga-DOTA-TOC

TABLE 1
Patient Data

Patient no.	Meningioma no.	Age (y)	Sex	Partial resection	Postoperative period (mo)	Meningioma volume (mL)	SUV
1	1	47	F	+	8	3.8	14.0
2	2	39	M	−		1.7	24.9
	3			−		0.9	4.2
	4			−		0.9	3.8
3	5	69	F	+	88	7.8	70.0
4	6	50	F	−		15.0	14.9
	7			−		45.0	3.4
5	8	81	F	−		4.0	6.6
	9			−		32.5	18.2
6	10	49	F	+	84	3.8	6.7
7	11	48	F	+	72	1.0	3.7
8	12	28	F	+	82	0.5	2.1
9	13	41	F	+	3	4.5	1.9
	14			−		32.0	7.3
	15			−		1.0	4.8
10	16	49	F	+	54	12.0	4.0
	17			−		0.6	2.9
11	18	45	F	+	3	24.0	12.3
12	19	64	F	+	60	3.9	3.8
13	20	57	F	+	90	18.2	8.5
14	21	64	F	+	97	4.0	3.0
15	22	50	F	+	3	1.6	3.9
16	23	25	F	+	3	12.0	29.0
17	24	42	M	+	11	1.1	1.8
18	25	52	F	−		5.3	6.6
19	26	48	F	+	4	24.9	6.4
20	27	53	F	−		20.1	19.8
21	28	62	F	−		86.0	6.4
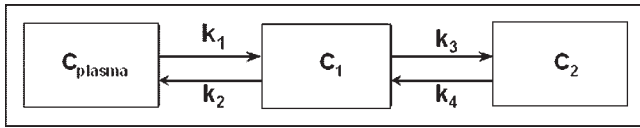
FIGURE 1. Two-tissue-compartment model with blood compartment.

could be eluted with ethanol. After evaporation of the organic solvent, the compound was redissolved in 5.0 mL of phosphate-buffered saline (0.01 mol/L; pH 7.4). The preparations were checked by paper chromatography (Whatman No. 1 paper; 55:45 methanol:acetate buffer [0.01 mL; pH 6.2]) for bound and free ^{68}Ga that remained at the start. Typically, more than 96% of the radioactivity migrated, with an R_f of ~0.6 corresponding to ^{68}Ga-DOTA-TOC.

Patients and Data Acquisition

Dynamic PET scans were acquired for 21 patients (mean age ± SD, 50.6 ± 12.9 y; 2 men and 19 women) with meningiomas (median grade I according to the system of the World Health Organization) before radiotherapy. Fifteen patients underwent partial resection 44.1 ± 39.4 mo, on average, before PET. To avoid partial-volume effects, we included only meningiomas with volumes of at least 0.5 mL from the total of 33 detected with PET ($n = 28$; mean volume, 13.1 mL). The patient data are shown in Table 1.

Written informed consent was obtained from all patients. The study was approved by the ethical committee of the University of Heidelberg.

After acquisition of transmission data (10 min, 3 ^{68}Ge line sources) to correct for attenuation, 155.7 ± 28.7 MBq of ^{68}Ga-DOTA-TOC were injected. Emission data were measured starting immediately after injection up to 60 min after injection (frames: 10 × 30 s, 5 × 60 s, 5 × 120 s, and 8 × 300 s). Measurements were obtained with a whole-body PET system, (ECAT EXACT HR$^+$; Siemens/CTI) covering 155 mm in the axial field of view (63 transversal slices, each 2.4 mm thick). Data were acquired in the 3-dimensional mode without interslice tungsten septa. This acquisition mode was selected because the total true-event sensitivity is higher by a factor of nearly 4.9 in the 3-dimensional mode than in the 2-dimensional mode (12). Quantification in 3-dimensional mode was found to be equivalent to that in 2-dimensional mode for the radioactivities used clinically. In 3-dimensional mode, the transaxial resolution ranges from 4.1 to 4.8 mm over a transaxial field of view of 400 mm (12,13). The matrix size was 128 × 128 pixels. Images were corrected for scatter and attenuation. Iterative image reconstruction used the ordered-subsets expectation maximization algorithm.

Data Analysis

For evaluation of the ^{68}Ga-DOTA-TOC kinetics, the rate constants k1, k2, k3, and k4 (dimensions, 1/min) and the vascular fraction (vB, vessel density as parameter that modulates uptake and improves the model) were computed using the PMod software (PMod Technologies Ltd.) (14). Furthermore, k1 − k1 × k2 (receptor binding) and the k1/k2 and k3/k4 ratios were calculated. The input function was retrieved from the image data. Time–activity curves were created using volumes of interest obtained from an arterial vessel. A 2-tissue-compartment model consisting of a blood compartment and 2 sequential tissue compartments is

commonly used for receptor studies. C_1 represents tracer specifically bound to the SSTR2, and C_2 represents tracer internalized into meningioma cells (Fig. 1). k1 describes the binding to the receptor, k2 the displacement from the receptor, k3 the cellular internalization, and k4 the externalization.

To determine the global uptake, standardized uptake values (SUVs) were determined:

$$SUV = \frac{\text{tissue activity concentration (kBq/g)}}{\text{injected dose (kBq)/body weight (g)}}.$$

Nasal mucosa, consistently showing a slight to moderate physiologic SSTR density, was chosen as the reference tissue (RT) (15). Mean SUVs in regions of interest, placed over meningiomas, nasal mucosa, and brain tissue in both temporal lobes, were calculated.

RESULTS

All meningiomas demonstrated a high tracer uptake and could clearly be separated from surrounding brain and bone (Fig. 2A). Uptake in meningiomas was biphasic, with a rapid increase during the first 10 min after tracer administration followed by a slower increase during the remaining examination time (Fig. 2B).
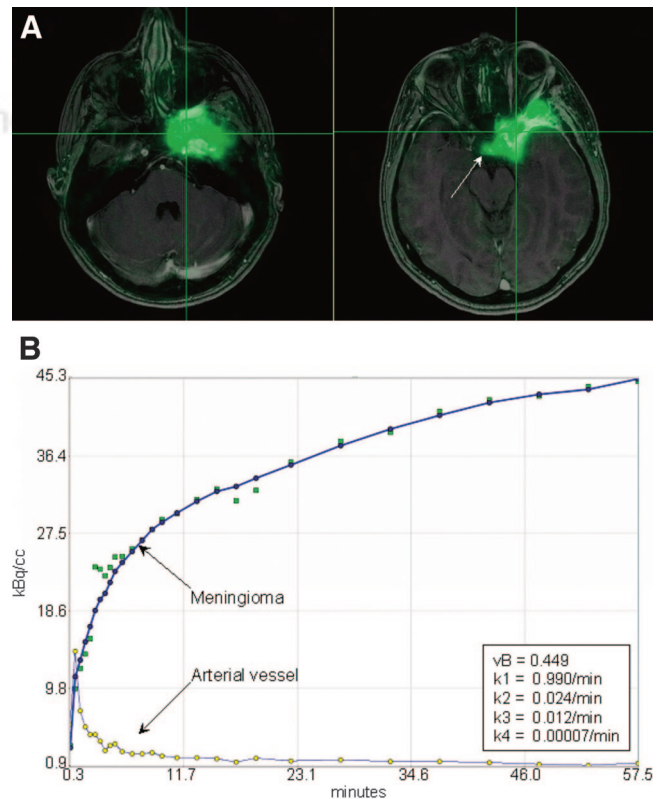
FIGURE 2. (A) Transaxial fusion images (gadolinium-DTPA–enhanced MRI in black and white; ^{68}Ga-DOTA-TOC PET in green) show high tracer uptake by meningioma in left sphenoid wing, with infiltration into left cavernous sinus and physiologic uptake by pituitary gland (arrow). (B) Fitted time–activity curves are shown for volumes of interest covering meningioma and an arterial vessel. Corresponding kinetic parameters of meningioma were calculated with PMod software.
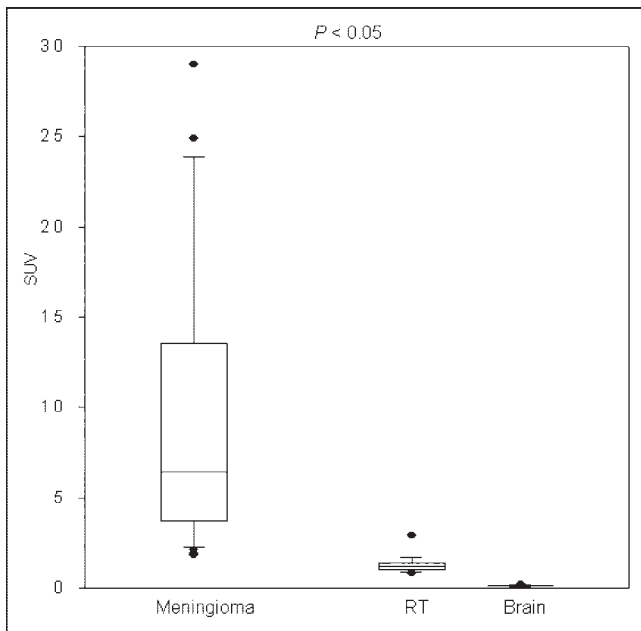
FIGURE 3. Box plots of SUVs for meningiomas, RT, and normal brain tissue. Boundary of box closest to zero indicates 25th percentile, line within box indicates median, and boundary of box farthest from zero indicates 75th percentile. Whiskers above and below box indicate 90th and 10th percentiles. Outlying values are graphed as dots.

Because of the intact blood–brain barrier, ^{68}Ga-DOTA-TOC did not accumulate in the surrounding brain tissue. Between 45 and 60 min after injection, mean SUV in normal brain tissue was 0.12 ± 0.04. In the same period, mean SUV was 10.5 ± 13.7 in meningiomas, 4.1 ± 2.1 in pituitary glands, and 1.3 ± 0.5 in RT. SUVs in meningiomas and their tumor volumes are given in Table 1. There was no correlation between these 2 parameters. SUVs were significantly higher in meningiomas than in RT and normal brain tissue ($P < 0.05$). The box plots in Figure 3 show the median, 10th, 25th, 75th, and 90th percentiles of SUV.

In meningiomas, a linear correlation between SUV and the k1/k2 ratio was found ($r = 0.77$; $P < 0.0001$; SUV = $2.20 + 0.75 \times$ [k1/k2]). There was also a linear correlation between the k3/k4 ratio and SUV ($r = 0.83$; $P < 0.0001$; SUV = $3.67 + 0.28 \times$ [k3/k4]). No correlation between

TABLE 2
Mean Values and SDs for vB, RB, k1, k2, k3, and k4 for RT and Meningiomas

Parameter	RT		Meningioma	
	Mean	SD	Mean	SD
vB	0.110	0.124	0.424	0.282
RB	0.130	0.091	0.486	0.321
k1	0.401	0.236	0.540	0.330
k2	0.556	0.292	0.117	0.160
k3	0.061	0.050	0.024	0.032
k4	0.080	0.176	0.004	0.007

SUV and vB or single parameters for k1, k2, k3, or k4 was detected in meningiomas.

Significant ($P < 0.05$) differences in meningiomas versus RT were found for vB (0.42 vs. 0.11), k2 (0.12 vs. 0.56), k3 (0.024 vs. 0.060), k4 (0.004 vs. 0.080), and RB (0.49 vs. 0.13). However, there was no significant difference for k1 (0.54 vs. 0.40). Mean values and SDs are given in Table 2. The mean ratios k1/k2 (4.50 vs. 0.71) and k3/k4 (6.00 vs. 0.75) were 6- to 8-fold higher in meningiomas than in RT.

The corresponding box plots are shown in Figure 4 for vB and RB; in Figure 5 for k1, k2, and k1/k2 ratio; and in Figure 6 for k3 and k4.

DISCUSSION

In an initial study of ^{68}Ga-DOTA-TOC in meningiomas, at 10 min after injection about 80% of the ^{68}Ga-DOTA-TOC
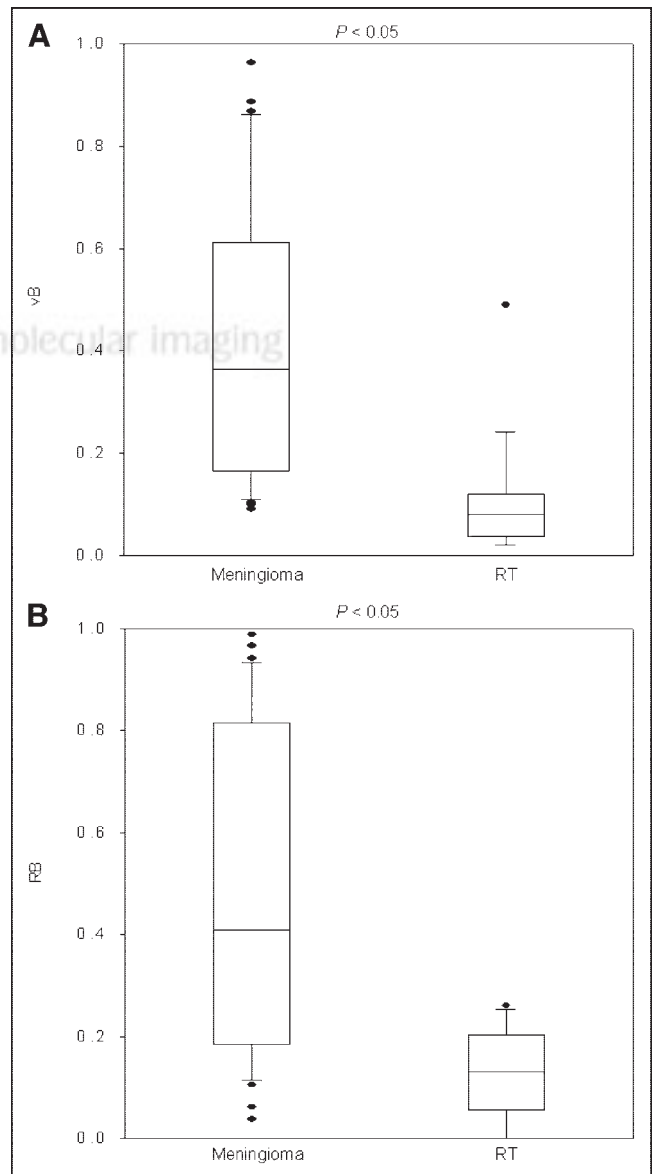
FIGURE 4. Box plots of vB (A) and RB (B) for meningiomas and RT.
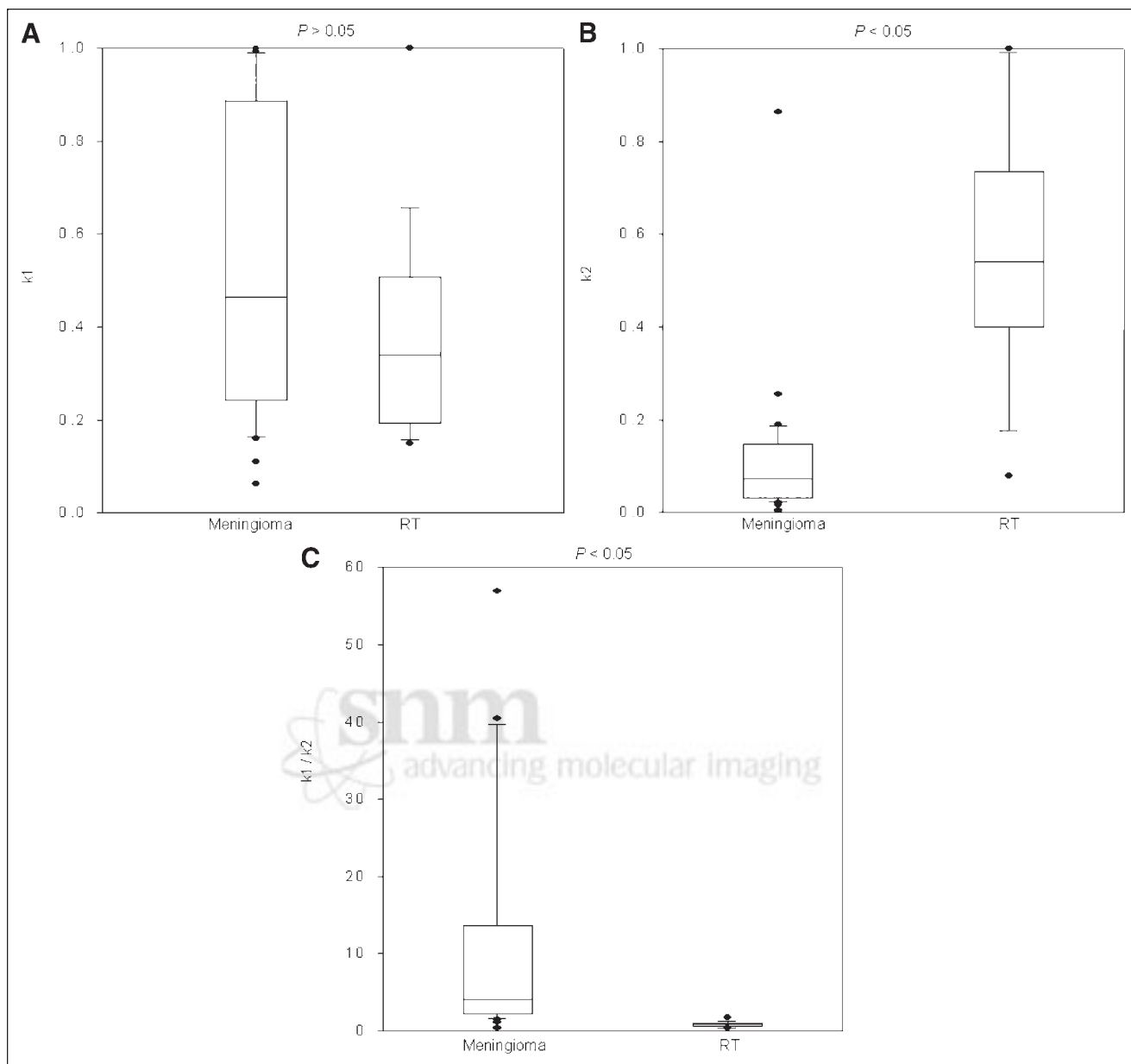
FIGURE 5. Box plots of k1 (A), k2 (B), and k1/k2 (C) for meningiomas and RT.

had rapidly cleared from blood because of extravasation, with a α-$t_{1/2}$ of 3.5 min (renal clearance not included). Renal clearance of the compound showed a β-$t_{1/2}$ of 63 min. The uptake in meningiomas increased rapidly after injection. The highest SUVs were found at a plateau between 60 and 120 min, with a mean of 10.5 ± 13.7. Because of the intact blood–brain barrier, no accumulation of ^{68}Ga-DOTA-TOC in the surrounding brain tissue (mean SUV, 0.12 ± 0.04) was found later than 10 min after injection (*10*). Labeling of DOTA-TOC with the generator nuclide ^{68}Ga is inexpensive and easy, and a titanium dioxide–based [68]Ge/^{68}Ga generator is commercially available.

The present study revealed significant differences between meningiomas and RT for SUV (mean, 10.5 vs. 1.3),

vB (0.42 vs. 0.11), k2 (0.12 vs. 0.56), k3 (0.024 vs. 0.061), k4 (0.004 vs. 0.080), and RB (0.49 vs. 0.13). However, the difference for k1 (0.54 vs. 0.40) was not significant. The ratios k1/k2 (4.50 vs. 0.71) and k3/k4 (6.00 vs. 0.75) were 6- to 8-fold higher in meningiomas than in RT. The high uptake of ^{68}Ga-DOTA-TOC in meningiomas is determined by high values for vB and RB and by high ratios for k1/k2 and k3/k4. In contrast, k2 (describing the displacement from the receptor) and k4 (describing the cellular externalization) were remarkably low. These data are evidence that the binding to the receptor and trapping by internalization are the mechanisms responsible for tracer accumulation. The parameters k1–k4, vB, and RB might serve as a basis for addressing issues such as differentiation of tumor entities at

FIGURE 6. Box plots of k3 (A) and k4 (B) for meningiomas and RT.

detected subtype in benign meningiomas (*18,19*). In 20 meningiomas, expression of messenger RNA for the 5 SSTRs was characterized by Northern blot and reverse transcriptase polymerase chain reaction analysis, which revealed all examined tumors to be positive for SSTR2 messenger RNA (*2*).

Furthermore, our patient data are in accordance with the high SSTR2 affinity of ^{68}Ga-DOTA-TOC and with its previously reported stable receptor binding in vitro (*5,6*) and its high cellular internalization rates. Froidevaux et al. demonstrated that ^{67}Ga-DOTA-TOC was strongly internalized by AR4-2J cells and that radioactivity dissociated only slowly from the cells after internalization (*20*).

Because biopsy has a high risk of hemorrhage, alternative methods for characterization of meningioma aggressiveness and tendency to progress are sought. This SSTR imaging technique may be applied clinically to improve the characterization of skull-base tumors when MRI findings are unclear and the tumor is to be treated by radiosurgery alone or stereotactic biopsy is risky for the patient. ^{68}Ga-DOTA-TOC PET adds valuable information on the extent of meningiomas beneath osseous structures, especially at the skull base. This information can be improved by fusing these functional images with morphologic images using either appropriate hardware such as PET/CT scanners or specially designed software. Large meningiomas at the base of the skull are difficult to treat because of their proximity or adherence to critical structures. The long-term results (median follow-up period, 35 mo) of a study on 189 patients with benign meningiomas demonstrated that fractionated stereotactic radiotherapy is safe and effective for meningiomas that are not totally resected or are unresectable (*21*). As will be evaluated in further studies, ^{68}Ga-DOTA-TOC PET might be helpful in the planning of stereotactic radiotherapy to delineate the extent of meningiomatous manifestation.

In the follow-up of patients after stereotactic radiotherapy, a distinction between scar tissue and radiation necrosis or meningioma recurrence significantly affects individual patient management (*3*). Further studies need to evaluate the clinical impact on follow-up after stereotactic radiotherapy of kinetic modeling using ^{68}Ga-DOTA-TOC, which might be more sensitive and specific than SUV or MRI alone.

the skull base, meningioma subtypes, meningioma grading, or postradiotherapy follow-up that has to be done in further studies.

Overall, our PET findings were in accordance with known histopathologic properties of benign meningiomas, such as high vascularization and high SSTR2 density. In a total of 40 intracranial meningiomas, classified as benign ($n = 31$), atypical ($n = 7$), and anaplastic ($n = 2$), microvessel density was immunohistochemically investigated. Most grade I meningiomas showed multiple large vessels, whereas grade II or III meningiomas showed small microvessels (*16*). In contrast to glioblastomas, benign meningiomas show a positive correlation between vascularization and tumor volume (*17*). Meningiomas express SSTRs in nearly 100% of cases, and SSTR2 is the most frequently

CONCLUSION

The high uptake of ^{68}Ga-DOTA-TOC in meningiomas, compared with RT, is in accordance with the high values for vB, k1/k2 ratio, k3/k4 ratio, and RB and with the remarkably low values for k2 and k4. Modeling of dynamic PET studies provides insight into the biologic properties of meningiomas. In further studies, these data might serve as a basis for therapy planning and monitoring of SSTRs after radiotherapy of meningiomas.

ACKNOWLEDGMENTS

REFERENCES

1. Black P. Meningiomas. In: Black P, Loeffler JS, eds. *Cancer of the Nervous System.* Oxford, U.K.: Blackwell Science; 1997:349–362.

2. Dutour A, Kumar U, Panetta R, et al. Expression of somatostatin receptor subtypes in human brain tumors. *Int J Cancer.* 1998;76:620–627.

3. Schmidt M, Scheidhauer K, Luyken C, et al. Somatostatin receptor imaging in intracranial tumors. *Eur J Nucl Med.* 1998;25:675–686.

4. Bohuslavizki KH, Brenner W, Braunsdorf WE, et al. Somatostatin receptor scintigraphy in the differential diagnosis of meningioma. *Nucl Med Commun.* 1996;17:302–310.

5. Heppeler A, Froidevaux S, Mäcke HR, et al. Radiometal-labelled macrocyclic chelator-derivatised somatostatin analogue with superb tumor-targeting properties and potential for receptor-mediated internal radiotherapy. *Chem Eur J.* 1999;7:1974–1981.

6. Reubi JC, Schär JC, Waser B, et al. Affinity profiles for human somatostatin receptor subtypes SST1-SST5 of somatostatin radiotracers selected for scintigraphic and radiotherapeutic use. *Eur J Nucl Med.* 2000;27:273–282.

7. Kowalski J, Henze M, Schuhmacher J, Mäcke HR, Haberkorn U. Evaluation of PET imaging using ^{68}Ga-DOTA-D Phe[1]-Tyr[3]-octreotide (DOTA-TOC) in comparison to ^{111}In-DTPAOC (Octreoscan): first results in patients with neuroendocrine tumors. *Mol Imaging Biol.* 2003;5:42–48.

8. Hofmann M, Maecke H, Börner AR, et al. Biokinetics and imaging with the somatostatin receptor PET radioligand [^{68}Ga] DOTA-TOC: preliminary data. *Eur J Nucl Med.* 2001;28:1751–1757.

9. Henze M, Schuhmacher J, Dimitrakopoulou-Strauss A, et al. Exceptional increase in somatostatin receptor expression in pancreatic neuroendocrine tumor, visualised with ^{68}Ga-DOTA-TOC-PET. *Eur J Nucl Med.* 2004;31:466.

10. Henze M, Schuhmacher J, Hipp P, et al. PET imaging of SSTR using [^{68}Ga]-DOTA-D Phe[1]-Tyr[3]-octreotide (DOTA-TOC): first results in meningioma-patients. *J Nucl Med.* 2001;42:1053–1056.

11. Schuhmacher J, Maier-Borst W. A new ^{68}Ge/^{68}Ga radioisotope generator system for production of ^{68}Ga in dilute HCl. *Int J Appl Radiat Isot.* 1981;32:31–36.

12. Brix G, Zaers J, Adam LE, et al. Performance evaluation of a whole-body PET scanner using the NEMA protocol. *J Nucl Med.* 1997;38:1614–1623.

13. Adam LE, Zaers J, Ostertag H, et al. Performance evaluation of the whole-body PET scanner ECAT EXACT HR$^+$ following the IEC standard. *IEEE Trans Nucl Sci.* 1997;44:1172–1179.

14. Mikolajzyk K, Szabatin M, Rudnicki P, Grodzki M, Burger C. A JAVA environment for medical image data analysis: initial application for brain PET quantification. *Med Inform.* 1998;23:207–214.

15. Neumann I, Mirzaei S, Birck R, et al. Expression of somatostatin receptors in inflammatory lesions and diagnostic value of somatostatin receptor scintigraphy in patients with ANCA-associated small vessel vasculitis. *Rheumatology.* 2004;43:195–201.

16. Pistolesi S, Boldrini L, Gisfredi S, et al. Angiogenesis in intracranial meningiomas: immunohistochemical and molecular study. *Neuropathol Appl Neurobiol.* 2004;30:118–125.

17. Principi M, Italiani M, Guiducci A, et al. Perfusion MRI in the evaluation of the relationship between tumor growth, necrosis and angiogenesis in glioblastomas and grade 1 meningiomas. *Neuroradiology.* 2003;45:205–211.

18. Schulz S, Pauli SU, Schulz S, et al. Immunohistochemical determination of five somatostatin receptors in meningioma reveals frequent overexpression of somatostatin receptor subtype sst2A. *Clin Cancer Res.* 2000;6:1865–1874.

19. Arena S, Barbieri F, Thellung S, et al. Expression of somatostatin receptor mRNA in human meningiomas and their implication in in vitro antiproliferative activity. *J Neurooncol.* 2004;66:155–166.

20. Froidevaux S, Eberle AN, Christe M, et al. Neuroendocrine tumor targeting: study of novel gallium-labeled somatostatin radiopeptides in a rat pancreatic tumor model. *Int J Cancer.* 2002;98:930–937.

21. Debus J, Wuendrich M, Pirzkall A, et al. High efficacy of fractionated stereotactic radiotherapy of large base-of-skull meningiomas: long-term results. *J Clin Oncol.* 2001;19:3547–3553.